Time-optimal control of spin-1/2 particles with dissipative and generalized radiation-damping effects

M. Lapert,[3] E. Assémat,[1] Y. Zhang,[2] S. J. Glaser,[2] and D. Sugny[1,*]

[1]*Laboratoire Interdisciplinaire Carnot de Bourgogne (ICB), UMR 5209 CNRS-Université de Bourgogne, 9 Av. A. Savary, BP 47 870, F-21078 DIJON Cedex, France, and Team GECO, INRIA Saclay, France*

[2]*Department of Chemistry, Technische Universität München, Lichtenbergstrasse 4, D-85747 Garching, Germany*

[3]*Institut für Quanteninformationsverarbeitung, Universität Ulm, D-89069 Ulm, Germany*

(Received 11 February 2013; published 17 April 2013)

We analyze the time-optimal control of spin-1/2 particles with bounded field amplitudes in the presence of dissipative and radiation damping effects. Using tools of geometric optimal control theory, we determine different optimal syntheses for specific values of the system parameters. We show the nontrivial role of the effective radiation damping effect on the optimal control law.

DOI: 10.1103/PhysRevA.87.043417 PACS number(s): 32.80.Qk, 37.10.Vz, 78.20.Bh

I. INTRODUCTION

Nuclear magnetic resonance (NMR) [1–3] is one of the most promising fields of applications of quantum control [4–7]. In this domain, optimal control techniques can be used to design magnetic fields to control the dynamics of spin systems with applications extending from quantum computing to spectroscopy [8]. Numerical optimization procedures such as the GRAPE algorithm (gradient ascent pulse engineering algorithm) [9,10] or the Krotov algorithm [11] have been developed to solve such control problems. Recently, methods of geometric optimal control theory [12–14] have also been applied with success in this field [15–21]. This approach, which is based on strong mathematical tools coming from differential geometry and Hamiltonian dynamics, has a rapid development permitting to attack problems of increasing difficulty. In this context, we have derived in Refs. [22–24] the complete solution of the optimal control of two-level dissipative quantum systems whose dynamics is governed by the Lindblad equation [25,26]. We have applied this analysis in [19] to control the saturation a spin-1/2 particle in a dissipative environment. In this paper, we propose to extend this work by studying the role of the radiation damping effect on the optimal control of the dynamics of a spin-1/2 particle [27–37]. In this setting, a preliminary experimental and numerical study has been done in [38] for the saturation control of a spin in minimum time.

Before entering into mathematical details of the analysis, we recall that, in NMR, the radiation damping effect arises during the measurement process of the magnetization [27–29]. This magnetization is measured by a coil, but the measured signal in this coil produces another magnetic field that influences the dynamics. This effect can be modeled by a nonlinear term in the Bloch equations of the dynamics. In this context, the question that naturally arises is the positive or negative role of these new terms on the optimal law. To be complete, we will analyze the double contribution of relaxation and radiation damping effects. The nonlinear effect is generally characterized by a positive radiation damping parameter. However, using radio-frequency feedback [30,31,33,39–41], the effect of radiation damping can be enhanced [32], suppressed [31,39], or even overcompensated [32], resulting in arbitrary effective radiation damping parameters that can be positive or negative. It is this general situation which will be considered in this work.

The paper is organized as follows. We first introduce the model for the dynamics of a spin-1/2 particle with relaxation and radiation damping effects. In Sec. III, we formulate the Pontryagin maximum principle (PMP) with a time minimum cost functional and we introduce the different geometric tools needed to solve the optimal control problem. Section IV is devoted to the computation of different optimal syntheses for specific values of the relaxation and radiation damping parameters. Conclusions and prospective views are given in Sec. V. Some technical computations are reported in Appendix.

II. THE MODEL SYSTEM

In this section, we introduce the nonlinear Bloch equation that is used in this paper. This model describes the magnetization of a sample in an NMR experiment with a nonlinearity arising from the interaction of the sample with the coil and experimental feedback. Assuming that the radio-frequency magnetic field is resonant with respect to the frequency of the spin-1/2 particle, the nonlinear Bloch equation is given in the corresponding rotating frame by [27,28]

$$\begin{aligned}\frac{dM_x}{dt} &= \omega_{1y}M_z - \frac{M_x}{T_2} - \frac{M_xM_z}{\tau_r M_0},\\ \frac{dM_y}{dt} &= -\omega_{1x}M_z - \frac{M_y}{T_2} - \frac{M_yM_z}{\tau_r M_0},\\ \frac{dM_z}{dt} &= -\omega_{1y}M_x + \omega_{1x}M_y - \frac{M_z - M_0}{T_1} + \frac{M_x^2 + M_y^2}{\tau_r M_0},\end{aligned} \tag{1}$$

where the M_i values are the coordinates of the magnetization vector $\vec{M}$ in the i direction and ω_{1i} the two components of the rf control field $\vec{\omega}$, which satisfies the constraint $|\vec{\omega}| \leqslant \omega_{\max}$. The two constants T_1 and T_2 are two relaxation rates describing the interaction of the system with the environment. M_0 is the thermal equilibrium magnetization, and τ_r is the effective radiation damping rate which can be positive or negative.

*dominique.sugny@u-bourgogne.fr

Note that without dissipation the norm of the magnetization vector is constant. To simplify the notations, we introduce the normalized coordinates $\vec{x} = \vec{M}/M_0$, the normalized control field $\vec{u} = 2\pi\vec{\omega}/\omega_{\max}$, and the normalized time $\tau = (\omega_{\max}/2\pi)t$ [19]. The dynamics is then ruled by the following system of differential equations:

$$\begin{aligned} \dot{x} &= -\Gamma x + u_2 z - kxz \\ \dot{y} &= -\Gamma y - u_1 z - kyz \\ \dot{z} &= \gamma(1-z) + u_1 y - u_2 x + k(x^2+y^2), \end{aligned} \tag{2}$$

where $\Gamma = 2\pi/(\omega_{\max}T_2)$, $\gamma = 2\pi/(\omega_{\max}T_1)$ and $k = 2\pi/(\omega_{\max}\tau_r M_0)$. As mentioned above, we assume that the parameter k can be positive or negative [39], while the dissipative parameters are positive. We will see that completely different behaviors are obtained according to the sign of the parameter k.

The goal of this work consists in solving the time-optimal control problem in the presence of relaxation and radiation damping effects. The initial state will be the thermal equilibrium point, while the final state can be any point of the reachable set. We will construct the optimal synthesis, i.e., the set of all the optimal solutions starting from the initial point and reaching any final state. We begin the analysis by first using the symmetry of revolution of the system around the z axis. Observe that the nonlinear term does not break this symmetry. Roughly speaking, if the initial state is on the z axis, which is usually the case in NMR when the initial point is the equilibrium point, then all the meridian planes containing the z axis are equivalent. This point is rigorously shown in [22,23] in the situation where only the relaxation rates are taken into account and can be straightforwardly extended to the radiation damping case.

Since the optimal dynamics is confined in a plane, we can assume without loss of generality that $u_2 = 0$. We finally get the equations

$$\begin{aligned} \dot{y} &= -\Gamma y - kyz - uz \\ \dot{z} &= \gamma(1-z) + ky^2 + uy, \end{aligned} \tag{3}$$

where $u \equiv u_1$ is the control. The dynamical system can also be rewritten in a vectorial form as follows:

$$\dot{\vec{X}} = \vec{F}(\vec{X}) + u\vec{G}(\vec{X}), \tag{4}$$

where the vectors $\vec{X}$, $\vec{F}$, and $\vec{G}$ have respectively the coordinates (y,z), $[-\Gamma y - kyz, \gamma(1-z) + ky^2]$, and $(-z,y)$. The vector fields $\vec{F}$ and $\vec{G}$ are associated to the uncontrolled and controlled parts of the dynamics.

III. METHODOLOGY

A. Fixed points and vector fields

We give in this section a global geometric description of the dynamics. Whereas the standard Bloch equation admits only one fixed point corresponding to the north pole $(y = 0, z = 1)$ of the Bloch sphere if $u = 0$, the main consequence of the introduction of the nonlinearity is the creation of new fixed points. The dynamics can have at most three fixed points for some values of the parameters. These fixed points are given by the equations

$$\begin{aligned} -\Gamma y - kyz - uz &= 0 \\ \gamma - \gamma z + ky^2 + uy &= 0, \end{aligned} \tag{5}$$

where u is constant. Using Eqs. (5), one deduces that the solutions are given by the following polynomial of order 3:

$$\frac{k^2}{\gamma}y^3 + \frac{2ku}{\gamma}y^2 + \left(\Gamma + \frac{k\gamma + u^2}{\gamma}\right)y + u = 0. \tag{6}$$

The complete resolution of Eq. (6) is detailed in Appendix. In particular, we give sufficient conditions for the existence of three fixed points. This case is illustrated in Fig. 1 for $u = 0$, 2π, and -2π. The vector field $\vec{F} + u\vec{G}$ is also represented by means of small arrows showing its direction and its intensity in the (y,z) plane. Note the different local structures around the three fixed points.

B. Pontryagin maximum principle

Powerful mathematical tools have been developed [14] to study controlled systems on two-dimensional manifolds. In this section, we briefly introduce the main results needed to solve the time-optimal control problem. We recall that the control field satisfies the constraint $|u| \leqslant 2\pi$, which is equivalent in the reduced coordinates to the constraint $|\vec{\omega}| \leqslant \omega_{\max}$. Since the geometrical study of the linear system has already been carried out in [22–24], we focus in this paper on the changes induced on the geometrical sets by the nonlinear term.

The main tool used here is the Pontryagin maximum principle (PMP) [42], which states that the optimal trajectories are solutions of the system

$$\begin{aligned} \dot{\vec{x}} &= \frac{\partial H}{\partial p}(\vec{x},\vec{p},v), \quad \dot{\vec{p}} = -\frac{\partial H}{\partial x}(\vec{x},\vec{p},v), \\ H(\vec{x},\vec{p},v) &= \max_{|u|\leqslant 2\pi} H(\vec{x},\vec{p},u), \\ H(\vec{x},\vec{p},v) &= 0, \end{aligned} \tag{7}$$

where $H(\vec{x},\vec{p},u) = \vec{p}\cdot(\vec{F}(\vec{x}) + u\vec{G}(\vec{x})) + p_0$ with $\vec{p}$ and $p_0 \leqslant 0$, the adjoint states, which are not simultaneously equal to zero. In our case, the Hamiltonian is

$$H = -p_y(\Gamma y + kyz + uz) + p_z(\gamma - \gamma z + ky^2 + uy) + p_0.$$

Introducing the switching function

$$\Phi(\vec{x}) = \vec{p}\cdot\vec{G}(\vec{x})$$

and applying the PMP, one can deduce that if $\Phi \neq 0$, i.e., in the *regular* case, the control solution of Eq. (7) is $v = 2\pi \times \mathrm{sgn}[\Phi]$. The field v is said to be bang if Φ does not change sign and bang-bang if Φ vanishes in an isolated point with a nonzero derivative. On the other hand, if Φ vanishes on an interval $[t_1,t_2]$, the corresponding *singular* control u_s can be computed by imposing that the first and second derivatives of Φ with respect to time are zero. For the first derivative, one gets that

$$\dot{\Phi} = \vec{p}\cdot[\vec{F},\vec{G}],$$

where the commutator of two vector fields is defined by $[\vec{F},\vec{G}] = d\vec{F}/d\vec{x}\cdot\vec{G} - \vec{F}\cdot d\vec{G}/d\vec{x}$. Straightforward computations lead to

$$[\vec{F},\vec{G}] = (-\gamma - (\Gamma - \gamma)\gamma z - kz^2, (\gamma - \Gamma)\gamma z + kyz),$$

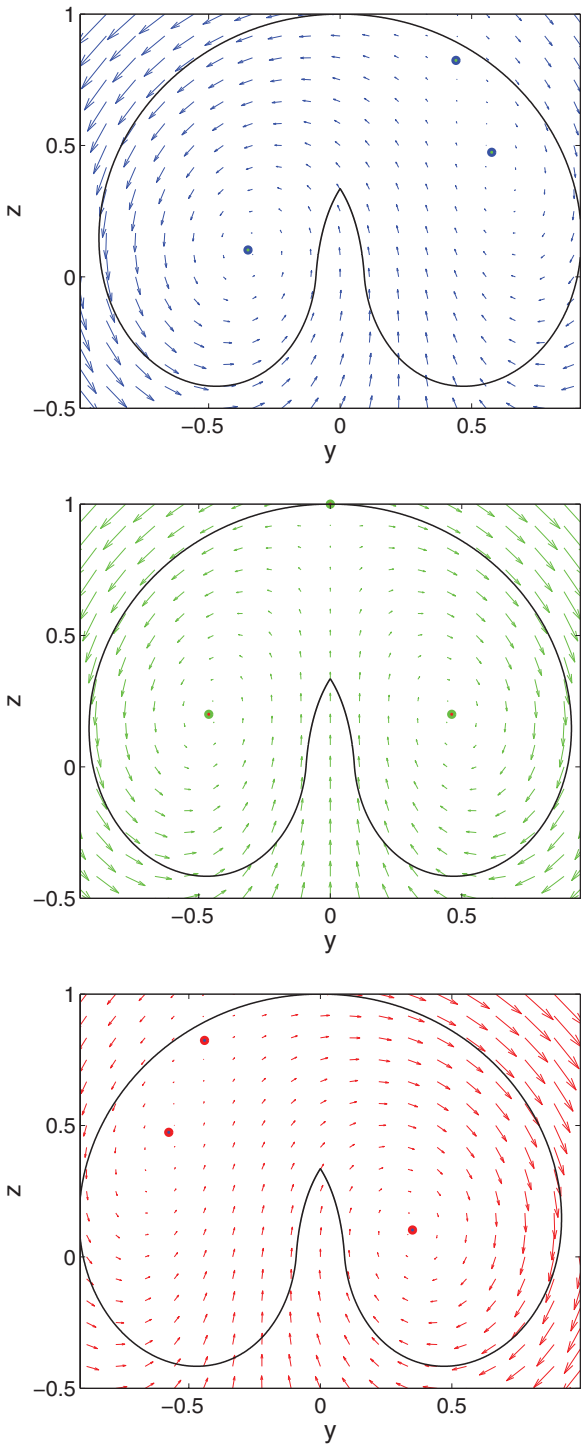

FIG. 1. (Color online) Global geometrical structure of the vector field $\vec{F}+u\vec{G}$ and distributions of the fixed points for $u=2\pi$ (top), $u=0$ (middle), and $u=-2\pi$ (bottom). The small arrows represent the direction and the modulus of $\vec{F}+u\vec{G}$ in the (y,z) plane. The dot corresponds to the fixed points of the controlled system. The solid line delimits the boundary of the reachable set for $|u|\leqslant 2\pi$. The different parameters are taken to be $\gamma=5.027$, $\Gamma=3.770$, and $k=-18.850$.

which depends on the parameter k. The functions Φ and $\dot{\Phi}$ can be simultaneously equal to 0 if and only if the vector fields $\vec{G}$ and $[\vec{F},\vec{G}]$ are parallel, giving the condition

$$\det(\vec{G},[\vec{F},\vec{G}])=y[\gamma+2(\Gamma-\gamma)\gamma z]=0,$$

independent of k. Finally, one obtains that the singular arcs, i.e., the trajectories for which the control is singular, belong to the set

$$S=\{\vec{x}\in\mathbb{R}^2/\det(\vec{G},[\vec{G},\vec{F}])(\vec{x})=0\}.$$

The set S is the union of the two lines of equation $y=0$ and $z=-\gamma/[2(\Gamma-\gamma)]$. The singular control field can be computed from the second time derivative of Φ:

$$\ddot{\Phi}=[\vec{G},[\vec{G},\vec{F}]]+u_s[\vec{F},[\vec{G},\vec{F}]]=0.$$

It can be shown that it depends on k:

$$u_s=\frac{2yz(\Gamma^2-\gamma^2)+\gamma y(2\gamma-\Gamma)}{2(\Gamma-\gamma)(y^2-z^2)-\gamma z}+k\frac{\gamma yz+2y\gamma(z^2-y^2)(\Gamma-\gamma)}{2(\Gamma-\gamma)(y^2-z^2)-\gamma z}. \tag{8}$$

Note that the singular control is equal to zero on the vertical singular line and depends on k only along the horizontal singular line:

$$u_s=\frac{\gamma(\gamma-2\Gamma)}{2\gamma(\Gamma-\gamma)}\frac{1}{y}+ky. \tag{9}$$

On the horizontal line, the domain where u_s is admissible, i.e., $|u_s|\leqslant 2\pi$, is given by

$$\left|\frac{\gamma(\gamma-2\Gamma)+2ky^2(\gamma-\Gamma)}{2(\Gamma-\gamma)y}\right|\leqslant 2\pi. \tag{10}$$

In the linear regime, the admissibility region is composed of two segments delimited by the extremity of the Bloch ball and by the point of coordinates $(y=\pm a,\ z=-\gamma/[2(\Gamma-\gamma)])$, where $a=\frac{\gamma(\gamma-2\Gamma)}{2\gamma(\Gamma-\gamma)}$. In the nonlinear case, the two limit points of admissibility close to the z axis transform into two points of coordinates:

$$y_\pm=\varepsilon\frac{2\pi\pm\sqrt{4\pi^2-4ak}}{2k};\quad z=-\frac{\gamma}{2(\Gamma-\gamma)}, \tag{11}$$

where $\varepsilon=\pm 1$ on the left and right parts of the z axis, respectively. For $k\ll 1$, the y_- solution tends to the limit points of admissibility of the linear case, $y=\pm a$, while the y_+ solution leaves the Bloch ball.

In the abnormal case where $p_0=0$, the condition $\Phi=0$ leads to the fact that the vectors $\vec{F}$ and $\vec{G}$ are collinear, which occurs on the set

$$C=\{\vec{x}\in\mathbb{R}^2/\det(\vec{F},\vec{G})(\vec{x})=0\}.$$

This collinear set, which satisfies

$$-\Gamma y^2+\gamma z(1-z)=0,$$

does not depend on k.

Every optimal trajectory is a concatenation of regular and singular arcs. We recall that the solutions computed from the PMP are only extremal solutions. Other tools have to be used to get global optimality results, like those introduced in [24] (see also [14] for a complete mathematical overview). Some examples will be given in Sec. IV.

IV. EXAMPLES OF OPTIMAL SYNTHESES

Optimal syntheses in the case of the dissipation alone ($k = 0$) have been completely described in [22–24]. We analyze here the changes produced by the nonlinear term in two specific examples of optimal syntheses, with $k > 0$ such that the system has only one fixed point and $k < 0$ such that the system has three fixed points. Other situations could be analyzed along the same lines. Note that some positive (resp. negative) values of k can be found for which the dynamics has three (resp. one) fixed points (see Appendix for the details).

We first consider a standard case studied for $k = 0$ in [19] and with $k \neq 0$ in [38]. This example corresponds to the saturation process in NMR, that consists in vanishing the magnetization vector $\vec{M}$ of a sample by using an adequate pulse sequence. As can be seen in Fig. 2, the optimal trajectory is a bang-singular-bang-singular pulse sequence, the singular control belonging to the vertical and the horizontal singular lines. The optimality character of this structure is proved mathematically in [23] and experimentally implemented in [19]. Here, we show the perturbative effect of the nonlinear term of the Bloch equation. The structure of the pulse sequence is unchanged and only a small deviation is observed between the two trajectories. This small difference has been obtained in all the other examples with the relevant physical positive parameter k that we have studied. This means that the radiation damping effect can be considered as a smooth perturbation if $k > 0$. This is no more the case when the system has three fixed points. The influence of the new fixed points on the structure of the optimal control can be seen in Fig. 3, which has a rich complexity explained below. The numerical parameters are set to be $\gamma = 5.027$, $\Gamma = 3.770$, $k = -18.850$. Using the results of Appendix, one deduces that this dynamical system has three fixed points for each constant value of u such that $|u| \leqslant 2\pi$. Moreover, since $\Gamma \leqslant \gamma$, the horizontal singular line of equation $z = -\gamma/[2(\Gamma - \gamma)]$ does not belong to the Bloch ball. This means that the optimal control field will be the concatenation of bang pulses and singular ones along the vertical axis. The optimal synthesis is represented in Fig. 3. The boundary of the reachable set is made of two bang-bang trajectories, a commutation occurring on the collinear locus as shown in [14]. Note that the center of the Bloch ball cannot be reached. Nine fixed points are plotted, the blue diamonds, the red dots, and the green stars corresponding to $u = 2\pi$, 0, and -2π, respectively. We also observe two particular lines, a switching curve in a red-dashed-dotted line and an overlap locus in green-dashed and blue-dotted lines. A switching curve is a curve such that the control field switches from $\pm 2\pi$ to $\mp 2\pi$ when the trajectory crosses this locus. An overlap curve is characterized by the fact that two different trajectories intersect with the same time duration on this curve. To highlight the role of this line, we consider two particular examples, which are depicted in Fig. 4. For instance, on the green-dashed curve, we use a bang-bang control along the AJI trajectory, while a bang-bang-bang-bang sequence corresponds to the AGHI curve. On the blue dotted overlap curve, we observe a bang-bang trajectory (points: AFK) which intersects with a bang-bang-singular-bang curve on the other side (points: AEDLK). The singular control here is a zero control along the vertical line. Due to the complexity of the analytical

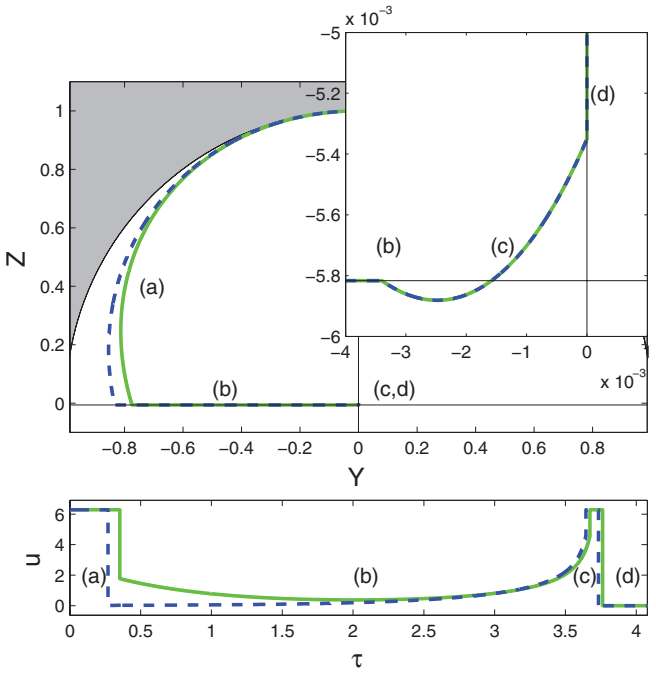

FIG. 2. (Color online) Optimal control for saturating a spin-1/2 particle (see the text for details). The dashed-blue (dark gray) and solid-green (light gray) lines depict, respectively, the cases $k = 0$ and $k = 2.260$. The relaxation parameters are set to $\Gamma = 1.346$ and $\gamma = 0.015$. The labels (a), (b), (c), and (d) indicate the different parts of the optimal trajectories. The inset is a zoom of the optimal curves near the center of the Bloch ball. The zone in gray is the exterior part of the Bloch ball. The different quantities are unitless.

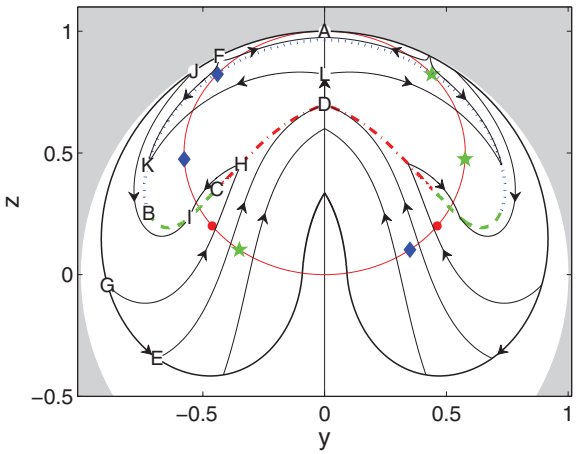

FIG. 3. (Color online) Optimal synthesis for the same set of parameters as Fig. 1. Different line types have been used to distinguish specific trajectories. The collinear set is plotted in red (dark gray). The blue diamonds, red dots, and green stars indicate the positions of the fixed points of the dynamics for $u = -2\pi$, $u = 2\pi$, and $u = 0$. The large black solid lines represent the boundary of the reachable set. The zone in gray is the exterior of the Bloch ball. The arrows indicate the direction in which the trajectories travel. The letters correspond to specific points which are used to describe the optimal curves (see the text for details).

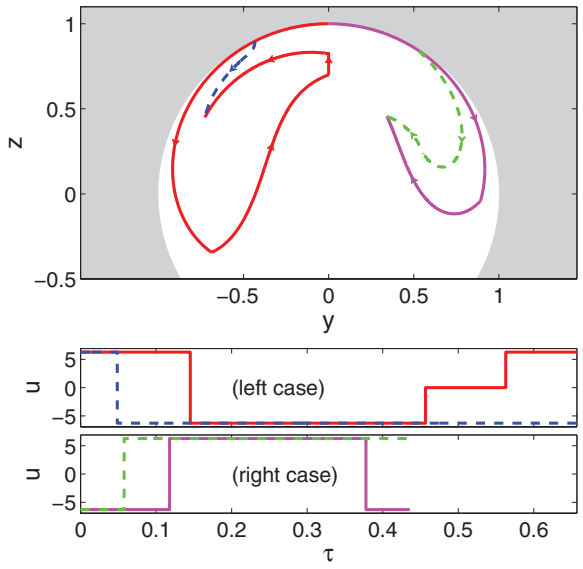

FIG. 4. (Color online) Same as Fig. 3 but only for the overlap curve. The two types of overlapping trajectories are plotted in the top panel (on the left and right sides of the z axis). Middle and bottom panels depict the control fields associated to the left and right trajectories, respectively. The same lines have been used for the trajectories (top) and the control fields (middle and bottom). The different quantities are unitless.

computations, note that we have found numerically all these optimal structures.

Some general comments can be made about the optimal synthesis. The first remark is based on the nature of the fixed points which can be hyperbolic as the one near the F point (blue diamond) [30]. In a neighborhood of this unstable equilibrium point, we observe the stable and unstable lines. The richness of the synthesis can also be seen from the different structures of optimal control extending from bang, bang-bang sequences with two or three switches and bang-bang-singular-bang.

V. CONCLUSION

We have investigated in this paper the time-optimal control of a spin-1/2 particle in the presence of radiation damping and relaxation effects. For different values of the system parameters, we have computed the optimal control laws, which shows the richness and the complexity of this optimal control problem. Such nontrivial behaviors are generally obtained in the case of a negative radiation damping effect, i.e., in the presence of a feedback magnetic field. It has been recently shown that the intensity and the phase of this field can be controlled [30]. In this framework, we have analyzed here the case of an arbitrary phase. This additional degree of freedom opens up in principle possible generalizations of our analysis.

This work can also be seen as an illustrative example of the efficiency of geometric optimal control theory to solve optimal control problems of low dimensions. When applicable, this approach is particularly interesting since it gives the global optimal solution for any point of the reachable set. This analysis completes the preceding works done in the past few years for which similar tools have been used to the control of dissipative two-level quantum systems [22–24] and to the control of a single spin-1/2 particle in the presence of relaxation. At this point, a natural question to ask is to which extent, in terms of size of the quantum system, this method could be applied. A first step in this generalization has been done for two uncoupled spins in [20,21]. We intend to pursue our efforts in this direction in the near future.

ACKNOWLEDGMENTS

S.J.G. acknowledges support from the DFG (GI 203/6-1), SFB 631. S.J.G. thanks the Fonds der Chemischen Industrie. D.S. and S.J.G. acknowledge support from the CCUFB and the French-German (Bayern) project on the optimal control of spin dynamics. D.S. acknowledges support from the PICS CNRS program.

APPENDIX: THE DYNAMICAL FIXED POINTS

We derive in this section the conditions satisfied by the fixed points of the nonlinear Bloch equation. We recall that such fixed points are solutions of

$$\frac{k^2}{\gamma}y^3 + \frac{2km}{\gamma}y^2 + \left(\Gamma + \frac{k\gamma + m^2}{\gamma}\right)y + m = 0, \quad \text{(A1)}$$

where the constant value of the field u is set to m. Dividing the left-hand side member of Eq. (A1) by k^2/γ, we introduce the three coefficients $b = 2m/k$, $c = \frac{(k\gamma+m^2+\gamma\Gamma)}{k^2}$, and $d = m\gamma/k^2$ of the polynomial and we denote by P the corresponding polynomial function. P has three real roots if the following

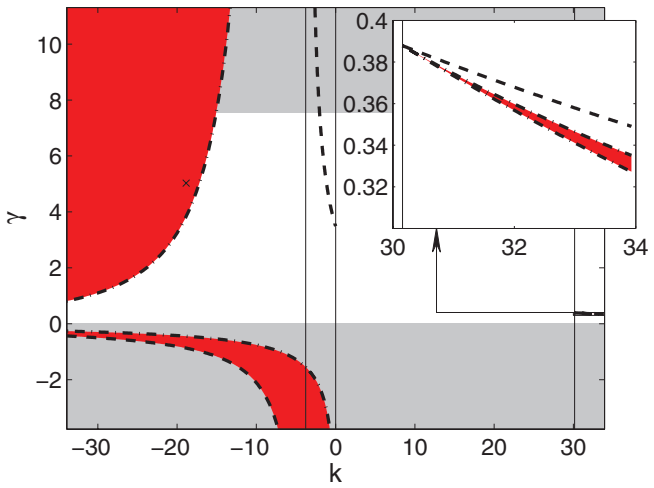

FIG. 5. (Color online) Set of parameters in red (dark gray) with three fixed points in the (γ,k) plane. The light-gray region represents the forbidden values of γ, and the white area depicts the set of parameters with only one fixed point. All the other lines correspond to conditions of existence of the three fixed points (see the text for details). The dashed and dashed-dotted lines are, respectively, the curves of equation $\gamma = m^2/(3(k+\Gamma))$ and $\gamma = \gamma_\pm$. The vertical black lines are, respectively, of equations $k = -\Gamma$, $k = 0$, and $k = 8\Gamma$. The insert is a zoom of the figure near the three fixed points area with positive k values (this zone is indicated by the arrow). Γ is set to 3.770 and m to 2π. The cross corresponds to the parameters used in Figs. 1, 3, and 4.

conditions are satisfied:

$$b^2 - 3c \geqslant 0, \tag{A2}$$

$$P(y_+)P(y_-) \leqslant 0, \tag{A3}$$

where $y_\pm = (-b \pm \sqrt{b^2 - 3c})/3$ are the roots of the derivative of P. The first condition is equivalent to

$$\begin{aligned} \gamma &\geqslant \frac{m^2}{3(k+\Gamma)} \quad \text{if} \quad k \leqslant -\Gamma, \\ \gamma &\leqslant \frac{m^2}{3(k+\Gamma)} \quad \text{if} \quad k \geqslant -\Gamma. \end{aligned} \tag{A4}$$

The equation of the dashed line of Fig. 5 is $\gamma = (m^2)/[3(k+\Gamma)]$. The equation $P(y_+)P(y_-) = 0$ can be written as follows:

$$27\gamma(a_1\gamma^2 + a_2\gamma + a_3)/k^6 = 0, \tag{A5}$$

with

$$\begin{aligned} a_1 &= 4(\Gamma + k)^3 \\ a_2 &= -20m^2\Gamma k + 8m^2\Gamma^2 - m^2k^2 \\ a_3 &= 4m^4\Gamma. \end{aligned} \tag{A6}$$

Let $\gamma_\pm$ and γ_0 be the three complex roots of the polynomial $a_1\gamma^3 + a_2\gamma^2 + a_3\gamma$. The three roots are real if the discriminant of $a_1\gamma^2 + a_2\gamma + a_3$ is positive, i.e., if $-m^4k(8\Gamma - k)^3 \geqslant 0$. This condition is equivalent to $k \notin [0, 8\Gamma]$. If $\gamma \leqslant k$, the parameter a_1 is negative and one deduces that the condition $P(y_+)P(y_-) \leqslant 0$ is fulfilled if $\gamma \notin [\gamma_-, \gamma_+]$. If $\gamma \geqslant k$, the parameter a_1 is positive and the relation $P(y_+)P(y_-) \leqslant 0$ is satisfied if $\gamma \in [\gamma_-, \gamma_+]$. We have therefore three fixed points if $\gamma \leqslant k$ and $\gamma \notin [\gamma_-, \gamma_+]$ or if $\gamma \geqslant k$ and $\gamma \in [\gamma_-, \gamma_+]$. Note that, in the case $\gamma = \gamma_\pm$, there is one fixed point and two degenerate fixed points. To summarize, we have the following results:

- Two fixed points if:

$$\gamma = \gamma_\pm \quad \text{and} \quad k \in [-\infty, -\Gamma] \cup [8\Gamma, +\infty]$$

- Three fixed points if:

$$\gamma \geqslant \frac{m^2}{3(k+\Gamma)}, \quad k \leqslant -\Gamma \quad \text{and} \quad \gamma \notin [\gamma_-, \gamma_+]$$

$$\gamma \leqslant \frac{m^2}{3(k+\Gamma)}, \quad k \in [-\Gamma, 0] \cup [8\Gamma, +\infty] \quad \text{and} \quad \gamma \in [\gamma_-, \gamma_+]$$

The region for which three fixed points exist is displayed in red (dark gray) in Fig. 5.

[1] M. H. Levitt, *Spin Dynamics: Basis of Nuclear Magnetic Resonance* (John Wiley and Sons, New York, 2008).

[2] R. R. Ernst, *Principles of Nuclear Magnetic Resonance in One and Two Dimensions*, International Series of Monographs on Chemistry (Oxford University Press, Oxford, UK, 1990).

[3] M. A. Bernstein, K. F. King, and X. J. Zhou, *Handbook of MRI Pulse Sequences* (Elsevier, Burlington, 2004).

[4] S. Rice and M. Zhao, *Optimal Control of Molecular Dynamics* (Wiley, New York, 2003).

[5] M. Shapiro and P. Brumer, *Principles of Quantum Control of Molecular Processes* (Wiley, New York, 2003).

[6] D. J. Tannor, *Introduction to Quantum Mechanics: A Time-Dependent Perspective* (University Science Books, Sausalito, CA, 2007).

[7] R. C. C. Brif and H. Rabitz, New J. Phys. **12**, 075008 (2010).

[8] N. C. Nielsen, C. Kehlet, S. J. Glaser, and N. Khaneja, *Optimal Control Methods in NMR Spectroscopy*, Encyclopedia of Nuclear Magnetic Resonance (Wiley, New York, 2010).

[9] N. Khaneja, T. Reiss, C. Kehlet, T. Shulte-Herbrüggen, and S. J. Glaser, J. Magn. Reson. **172**, 296 (2005); T. E. Skinner, T. O. Reiss, B. Luy, N. Khaneja, and S. J. Glaser, *ibid.* **163**, 8 (2003); **172**, 17 (2005); T. E. Skinner, K. Kobzar, B. Luy, R. Bendall, W. Bermel, N. Khaneja, and S. J. Glaser, *ibid.* **179**, 241 (2006); N. I. Gershenzon, K. Kobzar, B. Luy, S. J. Glaser, and T. E. Skinner, *ibid.* **188**, 330 (2007).

[10] P. de Fouquieres, S. G. Schirmer, S. J. Glaser, and I. Kuprov, J. Magn. Reson. **212**, 412 (2011).

[11] M. S. Vinding, I. I. Maximov, Z. Tosner, and N. C. Nielsen, J. Chem. Phys. **137**, 054203 (2012); I. Maximov, J. Salomon, G. Turinici, and N. C. Nielsen, *ibid.* **132**, 084107 (2010).

[12] B. Bonnard and M. Chyba, *Singular Trajectories and their Role in Control Theory* (Springer-Verlag, Berlin, 2003), Vol. 40.

[13] V. Jurdjevic, *Geometric Control Theory* (Cambridge University Press, Cambridge, UK, 1996).

[14] U. Boscain and B. Piccoli, *Optimal Syntheses for Control Systems on 2-D Manifolds* (Springer-Verlag, Berlin, 2004), Vol. 43.

[15] U. Boscain and P. Mason, J. Math. Phys. **47**, 062101 (2006).

[16] N. Khaneja, R. Brockett, and S. J. Glaser, Phys. Rev. A **63**, 032308 (2001).

[17] X. Chen, E. Torrontegui, D. Stefanatos, J.-S. Li, and J. G. Muga, Phys. Rev. A **84**, 043415 (2011); D. Stefanatos, J. Ruths, and J.-S. Li, *ibid.* **82**, 063422 (2010).

[18] D. Stefanatos, Phys. Rev. A **80**, 045401 (2009); D. Sugny and M. Joyeux, J. Chem. Phys. **112**, 31 (2000).

[19] M. Lapert, Y. Zhang, M. Braun, S. J. Glaser, and D. Sugny, Phys. Rev. Lett. **104**, 083001 (2010); **82**, 063418 (2010).

[20] M. Lapert, Y. Zhang, M. Janich, S. J. Glaser, and D. Sugny, Sci. Rep. **2**, 589 (2012).

[21] E. Assémat, M. Lapert, Y. Zhang, M. Braun, S. J. Glaser, and D. Sugny, Phys. Rev. A **82**, 013415 (2010).

[22] B. Bonnard, M. Chyba, and D. Sugny, IEEE Trans. Autom. Control **54**, 2598 (2009).

[23] B. Bonnard and D. Sugny, SIAM J. Control Optim. **48**, 1289 (2009).

[24] D. Sugny, C. Kontz, and H. R. Jauslin, Phys. Rev. A **76**, 023419 (2007).

[25] G. Lindblad, Commun. Math. Phys. **48**, 119 (1976).

[26] V. Gorini, A. Kossakowski, and E. C. G. Sudarshan, J. Math. Phys. **17**, 821 (1976).

[27] N. Bloembergen and R. V. Pound, Phys. Rev. **95**, 8 (1954).

[28] W. S. Warren, S. L. Hammes, and J. L. Bates, J. Chem. Phys. **91**, 5895 (1989).
[29] S. Bloom, J. Appl. Phys. **28**, 800 (1957).
[30] D. Abergel, A. Louis-Joseph, and J.-Y. Lallemand, J. Chem. Phys. **116**, 7073 (2002).
[31] A. Louis-Joseph, D. Abergel, and J.-Y. Lallemand, J. Biomol. NMR **5**, 212 (1995).
[32] D. Abergel, A. Louis-Joseph, and J.-Y. Lallemand, Chem. Phys. Lett. **262**, 465 (1996).
[33] D. Abergel, A. Louis-Joseph, and J.-Y. Lallemand, J. Chem. Phys. **112**, 6365 (2000).
[34] D. Abergel, Phys. Lett. A **302**, 17 (2002).
[35] M. Augustine, Prog. Nucl. Magn. Reson. Spectrosc. **40**, 111 (2002).
[36] M. Augustine, S. Bush, and E. Hahn, Chem. Phys. Lett. **322**, 111 (2000).
[37] A. Sodickson, W. E. Maas, and D. G. Cory, J. Magn. Reson., Ser. B **110**, 298 (1986).
[38] Y. Zhang, M. Braun, M. Lapert, D. Sugny, and S. J. Glaser, J. Chem. Phys. **134**, 054103 (2011).
[39] P. Broekaert and J. Jeener, J. Magn. Reson., Ser. A **113**, 60 (1995).
[40] J. Chen, B. Cutting, and G. Bodenhausen, J. Chem. Phys. **112**, 6511 (2000).
[41] C. Altafini, P. Cappelaro, and D. Cory, Systems Control Lett. **59**, 12 (2010).
[42] L. Pontryagin *et al.*, *Mathematical Theory of Optimal Processes* (Mir, Moscow, 1974).